The Internalization and Degradation of Human Copper Transporter 1 following Cisplatin Exposure

Alison K. Holzer and Stephen B. Howell

Department of Medicine and the Rebecca and John Moores Cancer Center, University of California at San Diego, La Jolla, California

Abstract

The human copper transporter 1 (hCTR1), the major transporter responsible for copper influx, mediates one component of the cellular accumulation of cisplatin (DDP). Both copper and DDP cause rapid down-regulation of hCTR1 expression in human ovarian carcinoma cells. In this study, we investigated the mechanism of this effect using digital deconvolution microscopy and Western blot analysis of cells stained with antibodies directed at both ends of the protein. Treatment of 2008 cells with DDP in combination with inhibitors of various endosomal pathways (amiloride, cytochalasin D, nystatin, and methyl-β-cyclodextrin) showed that hCTR1 degradation was blocked by amiloride and cytochalasin D, indicating that hCTR1 was internalized primarily by macropinocytosis. Expression of transdominant-negative forms of dynamin I and Rac showed that loss of hCTR1 was not dependent on pathways regulated by either of these proteins. DDP-induced loss of hCTR1 was blocked by the proteasome inhibitors lactacystin, proteasome inhibitor 1, and MG132. This study confirms that DDP triggers the rapid loss of hCTR1 from ovarian carcinoma cells at clinically relevant concentrations. The results indicate that DDP-induced loss of hCTR1 involves internalization from the plasma membrane by macropinocytosis followed by proteasomal degradation. Because hCTR1 is a major determinant of early DDP uptake, prevention of its degradation offers a potential approach to enhancing tumor sensitivity. (Cancer Res 2006; 66(22): 10944-52)

Introduction

The chemotherapeutic drug cisplatin (DDP) is important in the treatment of several types of cancer, including lung, testicular, ovarian, cervical, and head and neck tumors (1). One of the limiting factors in its use is the rapid development of resistance. Although the mechanism by which DDP enters the cell is poorly defined, emergence of resistance is commonly accompanied by decreased drug accumulation (reviewed in refs. 2–4). The major copper transporters have recently been shown to modulate the cellular accumulation of DDP (reviewed in ref. 5). Both copper and DDP are highly polar, and their uptake is influenced by similar extracellular factors, such as potassium ion concentration, pH, and the presence of reducing agents (4, 6). DDP resistance is often accompanied by cross-resistance to copper and vice versa (7, 8). We (9, 10) and others (11, 12) have shown that the major plasma membrane copper influx transporter, copper transporter 1 (CTR1), is responsible for a substantial portion of the DDP influx in both yeast and mammalian cells.

Copper homeostasis is maintained by highly conserved pathways that control the influx and efflux of copper. At the plasma membrane, CTR1 binds extracellular Cu^{+1} at its NH_2-terminal end and transports it across the plasma membrane. CTR1 then transfers the copper to one of several intracellular chaperones that protect Cu^{+1} from oxidation and delivers it to sites where it is required throughout the cell. The transfer of copper from CTR1 to a chaperone, such as ATOX1, and subsequently from a copper chaperone to a copper-requiring enzyme or efflux transporter is believed to involve a transchelation reaction that occurs through the intimate and specific interaction of the copper-binding proteins (13). This protein-protein interaction not only ensures that copper is selectively delivered to copper-requiring enzymes but also prevents copper from participating in nonspecific oxidation-reduction reactions.

Because of its potential to undergo oxidation-reduction cycling, copper is quite toxic to cells. One mechanism by which copper uptake is limited is through copper-induced down-regulation of CTR1 expression (14, 15). We have shown that DDP also triggers the rapid loss of human CTR1 (hCTR1) from the plasma membrane of human ovarian carcinoma cells (16). DDP is substantially more potent than copper, and the kinetics of the DDP-induced loss of hCTR1 are more rapid. That down-regulation of hCTR1 expression is functionally important was documented by showing that brief exposure to copper reduced DDP uptake and vice versa (16). The mechanism by which either copper or DDP causes the loss of hCTR1 is unknown but possibilities include simple relocalization from the plasma membrane to internal compartments, endocytosis followed by lysosomal degradation, proteasomal degradation, etc. Petris et al. (14) reported that inhibition of endocytosis with a chemical inhibitor, methyl-β-cyclodextrin, blocked the copper-induced loss of hCTR1 in mammalian cells that had been transfected with a hCTR1 expression vector. However, such high level expression of hCTR1 not only is toxic to cells but also seems to alter the normal trafficking of hCTR1 and its ability to deliver substrates to their normal destinations within the cell (16). We approached the challenge of determining the mechanism by which DDP triggers the disappearance of hCTR1 from human ovarian carcinoma cells by blocking endocytosis and proteasomal degradation separately using several different chemical agents and by using the expression of transdominant-negative variants of proteins that interfere with endocytosis. We report here that hCTR1 internalization and degradation following DDP exposure occurs through macropinocytosis followed by proteasomal degradation.

Note: Supplementary data for this article are available at Cancer Research Online (http://cancerres.aacrjournals.org/).

Presented in part at the 2005 meeting of the AACR.

Requests for reprints: Stephen B. Howell, Department of Medicine and the Rebecca and John Moores Cancer Center, University of California at San Diego, 3855 Health Sciences Drive, La Jolla, CA 92093-0819. Phone: 858-822-1110; Fax: 858-822-1111; E-mail: showell@ucsd.edu.

doi:10.1158/0008-5472.CAN-06-1710

Materials and Methods

Drugs and reagents. Platinol-AQ was a gift from Bristol-Myers Squibb (Princeton, NJ). The clinical formulation containing 3.33 mmol/L DDP was kept in the dark at room temperature. A 100 μmol/L stock was created by diluting the drug in 0.9% NaCl. Protein concentration was measured using Bradford's reagent from Bio-Rad, Inc. (Hercules, CA). The generation of the rabbit polyclonal antibody against amino acids 1 to 67 of hCTR1 used for immunofluorescence is described elsewhere (17). The polyclonal anti-rabbit antibody was generated by immunizing rabbits with a peptide containing amino acids from the COOH terminus of hCTR1 by Novus Biologicals (Littleton, CO). FITC-conjugated goat anti-rabbit antibody was obtained from Jackson ImmunoResearch Laboratories, Inc. (West Grove, PA). Hoechst 33342 dye for nuclear staining was purchased from Molecular Probes (Eugene, OR). Transferrin-Alexa Fluor 546 and 70-kDa dextran-Texas red were purchased from Molecular Probes. The polyclonal rabbit anti-hCTR1 antibody used for Western blotting was generated by immunizing rabbits with a peptide containing amino acids 2 to 22 of the NH_2 terminus of hCTR1 by BioCarta, Inc. (San Diego, CA). Horseradish peroxidase (HRP)–conjugated goat anti-rabbit secondary antibody was purchased from Amersham Pharmacia (Piscataway, NJ). All other chemicals and reagents were obtained from Fisher Scientific (Tustin, CA).

Cell lines and vectors. The 2008 ovarian carcinoma cells (18, 19) were grown in RPMI 1640 containing 10% fetal bovine serum (FBS) at 37°C in 5% CO_2. The HeLa cells engineered to express an inducible K44A dominant-negative mutant were used as described elsewhere (20). Ovarian carcinoma 2008 cells were transiently transfected with the Rac dominant-negative N17rac1 vector using LipofectAMINE (Invitrogen, Carlsbad, CA) according to the manufacturer's instructions.

Western blot analysis. Cells were grown in a T75 flask until 80% confluent and then exposed to DDP with or without inhibitors or medium alone for various times and at various concentrations. Following exposure, cells were harvested with trypsin and pelleted by centrifugation at 4°C. The pellet was frozen at −20°C for 1 hour and then thawed on ice and resuspended in 100 μL of homogenizing buffer [250 mmol/L sucrose, 10 mmol/L Tris-HCl (pH 7.4), 1 μg/mL antipain, 1 μg/mL pepstatin, 1 μg/mL leupeptin, 20 μg/mL phenylmethylsulfonyl fluoride] and homogenized using a dounce homogenizer for 1 minute. The suspension was centrifuged for 15 minutes at 500 × *g* at 4°C, and the protein content of the supernatant was measured. Supernatant samples containing 100 μg protein were boiled before electrophoresis in a 4% to 20% SDS-PAGE gel. Transfer to nitrocellulose membranes (Bio-Rad) was done electrophoretically for 30 minutes at 200 V using a Transblot SD apparatus (Bio-Rad). Membranes were blocked with 5% milk in TBS for 1 hour at room temperature. Blots were incubated at 4°C overnight with anti-hCTR1 antibody diluted 1:1,000 and mouse anti-tubulin (Sigma, St. Louis, MO) diluted 1:20,000 in 5% milk in TBS. Membranes were then washed thrice with TBS containing 0.05% Tween 20 and incubated with HRP-conjugated anti-mouse and anti-rabbit antibodies for 1 hour at room temperature. Before detection, membranes were again washed thrice with TBS containing 0.05% Tween 20 and detection was done using the enhanced chemiluminescence Western detection system from Amersham Pharmacia according to the manufacturer's instruction.

Deconvolution digital immunofluorescent microscopy. Cells were grown in a T75 flask until 80% confluent and then harvested with trypsin and pelleted by centrifugation in RPMI 1640 with 10% FBS. The resulting pellet was resuspended in 5 mL of RPMI 1640 containing 10% FBS, and 100 μL of cells were added to each well of a 24-well plate. Before the addition of cells, a 0.16-mm-thick coverslip and 300 μL of RPMI 1640 containing 10% FBS were placed in each well. Once cells became 80% confluent on the coverslip, at ~48 hours after plating, the cells were exposed to RPMI 1640 with 10% FBS containing either a chemical inhibitor or medium alone for 30 minutes (excluding amiloride that was added for 15 minutes) followed by the addition of 2 μmol/L DDP and either transferrin-Alexa Fluor 546 (25 μg/mL) or Texas red–labeled neutral dextran 70 (100 μg/mL) for 15 minutes. After the specified duration of exposure, the coverslips were placed at 4°C and washed thrice with PBS and then fixed in 3.7% formaldehyde in the same buffer at room temperature for 30 minutes. The images in each panel of the figures in this article are representative of three images taken from each of three independent experiments. Images are normalized to the autofluorescence of unstained 2008 cells, and cells were stained with only the secondary antibody.

Propidium iodide staining. 2008 ovarian carcinoma cells were grown to 80% confluency in 30-cm plates. Cells were then exposed to a range of inhibitors at varying concentrations for 30 minutes. The inhibitors and concentrations used are as follows: nystatin (0, 15, 30, and 50 μg/mL), methyl-β-cyclodextrin (0, 2, 3.5, and 5 mmol/L), cytochalasin D (0, 5, 10, and 20 μmol/L), cyclohexamide (0, 50, 100, and 150 μg/mL), lactacystin (0, 7, 14, and 20 μmol/L), proteasome inhibitor 1 (0, 7, 14, and 20 μmol/L), and MG132 (0, 14, 28, and 40 μmol/L). Cells were exposed to amiloride (0, 1, 2.5, and 5 mmol/L) for 15 minutes. Following exposure, cells were rinsed with PBS, trypsinized, and pelleted. The resulting pellet was rinsed with PBS and repelleted. The pellet was resuspended in 500 μL of 0.1% bovine serum albumin in PBS followed by the addition of 5 μL of propidium iodide (10 μg/mL). Membrane viability as determined by propidium iodide uptake was measured by fluorescence-activated cell sorting scanning. Repeated freezing-thawing and hydrogen peroxide treatment were used as positive controls. Each inhibitor concentration was done in triplicate. The concentration used for each inhibitor was based on the highest inhibitor concentration that maintained membrane viability.

Results

The level of expression of hCTR1 in 2008 human ovarian carcinoma cells was monitored using confocal digital deconvolution microscopic examination of cells immunohistochemically stained with an antibody specific for an epitope in the NH_2-terminal end of hCTR1. Cells were exposed to Texas red–labeled 70-kDa neutral dextran either alone or in combination with 2 μmol/L DDP for 15 minutes before staining. Neutral dextran of this molecular weight enters cells via a macropinocytotic process, and the uptake of this molecule served as a control (21, 22). As shown in Fig. 1*A*, in 2008 cells, hCTR1 was found both in the plasma membrane and in internal membranes of the cell. As shown in Fig. 1*A* (compare *left* and *right*), exposure of 2008 cells to DDP for 15 minutes caused complete disappearance of the green fluorescent hCTR1 signal but had no effect on the uptake of dextran as evidenced by persistence of the red signal. The DDP-induced loss of hCTR1 was not just due to relocalization from the plasma membrane to an interior cellular compartment as the hCTR1 signal disappeared from both sites. As we have previously reported (16), it was also not due to masking of the epitope detected by the antibody because identical results were obtained using cell lysates analyzed on denaturing and nondenaturing gels, and treatment of either lysates from previously untreated cells or the purified extracellular domain of hCTR1 with DDP did not reduce the ability of the anti-hCTR1 antibody to recognize epitopes on hCTR1. DDP-induced loss of CTR1 was also observed when the DDP-treated cells were stained with an antibody recognizing the COOH-terminal end of hCTR1. Thus, DDP triggers the disappearance of hCTR1 in cells that are proficient with respect to macropinocytosis.

To determine the mechanism by which DDP triggered the loss of hCTR1, we used both chemical inhibitors and expression of transdominant-negative variants of proteins known to inactivate endocytotic pathways. Several unique endocytotic pathways are now known, each of which depends on somewhat different protein complexes to manage the process of vesicle formation and release from the plasma membrane (reviewed in ref. 23). These pathways can be disabled by agents belonging to a variety of different chemical classes, although none of the drugs known to inhibit

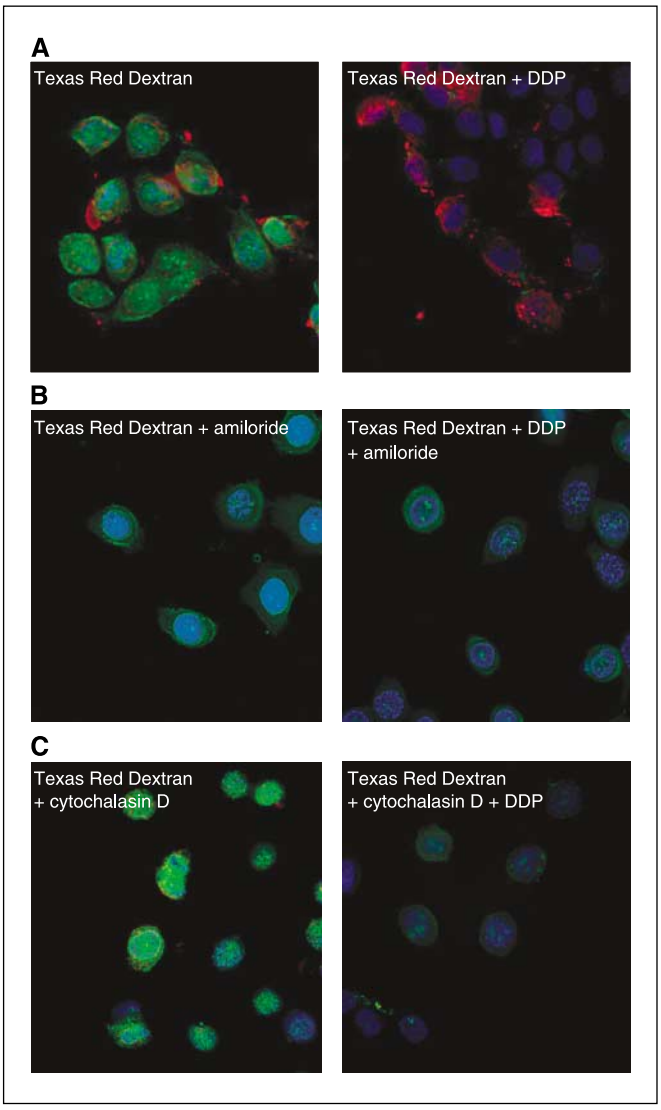

Figure 1. Confocal microscopic analysis of the effect of endocytotic pathway inhibitors amiloride and cytochalasin D on DDP-induced loss of hCTR1 from human ovarian carcinoma 2008 cells. In each case, following the indicated exposures, cells were stained for hCTR1 (*green*); Hoechst 33342 dye was used to label the nucleus (*blue*). *A,* untreated control cells incubated with Texas red–labeled dextran alone (*red; left*) and cells incubated with Texas red–labeled dextran and exposed to 2 μmol/L DDP for 15 minutes (*right*). *B,* cells incubated with Texas red–labeled dextran and 5 mmol/L amiloride for 15 minutes (*left*) and cells incubated with Texas red–labeled dextran, 5 mmol/L amiloride, and then 2 μmol/L DDP for 15 minutes (*right*). *C,* cells incubated with Texas red–labeled dextran and 10 μmol/L cytochalasin D for 30 minutes (*left*) and cells incubated with Texas red–labeled dextran and 10 μmol/L cytochalasin D for 30 minutes and then exposed to 2 μmol/L DDP for 15 minutes (*right*).

these pathways are entirely specific for any one endocytotic mechanism. Four agents widely used to study endocytotic pathways were selected for this study, including amiloride, cytochalasin D, nystatin, and methyl-β-cyclodextrin. For each agent, a concentration that produced inhibition of endocytosis in the absence of discernable cytotoxicity was identified by measuring both the inhibition of uptake of a fluorescent marker known to be endocytosed by the pathway targeted by the drug and the accumulation of propidium iodide as a function of concentration in 2008 cells. The use of each of these inhibitors altered the cellular levels of hCTR1 compared with untreated cells. Among the drugs that inhibit endocytosis, amiloride is one of the more specific agents in that it inhibits macropinocytosis without blocking other forms of pinocytosis or endocytosis (24). As shown in Fig. 1*B*, exposure of 2008 cells to 5 mmol/L amiloride for 15 minutes markedly reduced the uptake of neutral dextran, indicating that macropinocytosis was effectively inhibited. As shown in Fig. 1*B* (*right*), amiloride also largely blocked the DDP-induced loss of hCTR1. Western blot analysis verified that a 15-minute exposure to 2 μmol/L DDP induced complete disappearance of hCTR1 from 2008 membranes and that this effect of DDP was almost entirely blocked by concurrent exposure to amiloride (Fig. 2). This result was further confirmed using an antibody to the COOH-terminal end of hCTR1, which showed the same effect of amiloride (Supplementary Fig. S1). This result identifies macropinocytosis as being an important step in the DDP-induced down-regulation of hCTR1 expression.

Additional experiments were done with cytochalasin D, a drug that inhibits both macropinocytosis and micropinocytosis (24). As shown in Fig. 1 (compare *A* and *C*), as was the case with amiloride, cytochalasin D effectively blocked the uptake of neutral dextran. It also increased the level of hCTR1 expression in the absence of DDP exposure. Comparison of the DDP untreated and treated cells in Fig. 1*C* shows that it also partially blocked the DDP-induced loss of hCTR1, although the effect was of a smaller magnitude than that of amiloride. This was confirmed on Western blot analysis and through use of the antibody to the COOH-terminal end rather than NH_2-terminal end of hCTR1 (Supplementary Fig. S1). Thus, two drugs that inhibit macropinocytosis, presumably by different mechanisms, both reduced DDP-induced loss of hCTR1, providing further evidence for the importance of this pathway in at least the initial steps in hCTR1 degradation.

Nystatin binds to cholesterol in cell membranes and disrupts the formation and trafficking of caveolae. Cholera toxin enters cells largely via the caveolar pathway and is used as a marker of pathway flux (24). As shown in Fig. 3 (compare *left* of *A* and *B*), a 30-minute exposure to 30 μg/mL nystatin successfully blocked caveolar-mediated endocytosis as shown by the lack of Alexa Fluor 555–labeled cholera toxin B accumulation in the nystatin-treated 2008

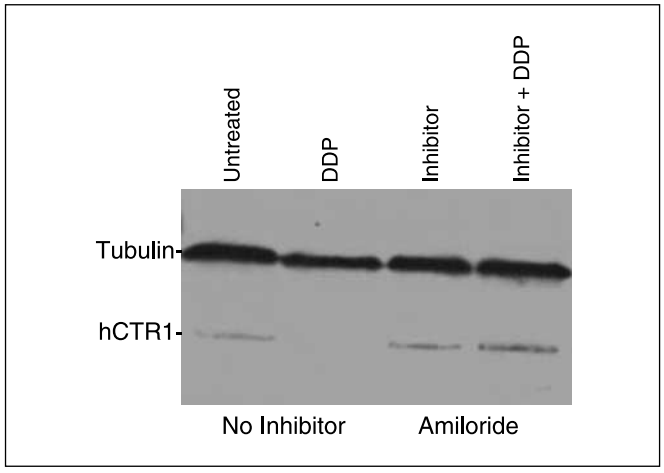

Figure 2. Western blot analysis of the effect of chemical inhibitors of endocytosis on hCTR1 loss following exposure to 2 μmol/L DDP for 15 minutes. Ovarian carcinoma 2008 cells were treated as described in Fig. 1. Denaturing Western blot showing the expression of tubulin and hCTR1 following exposure to amiloride alone or amiloride in combination with DDP. Blot is representative of three independent analyses done with lysates from three independent experiments.

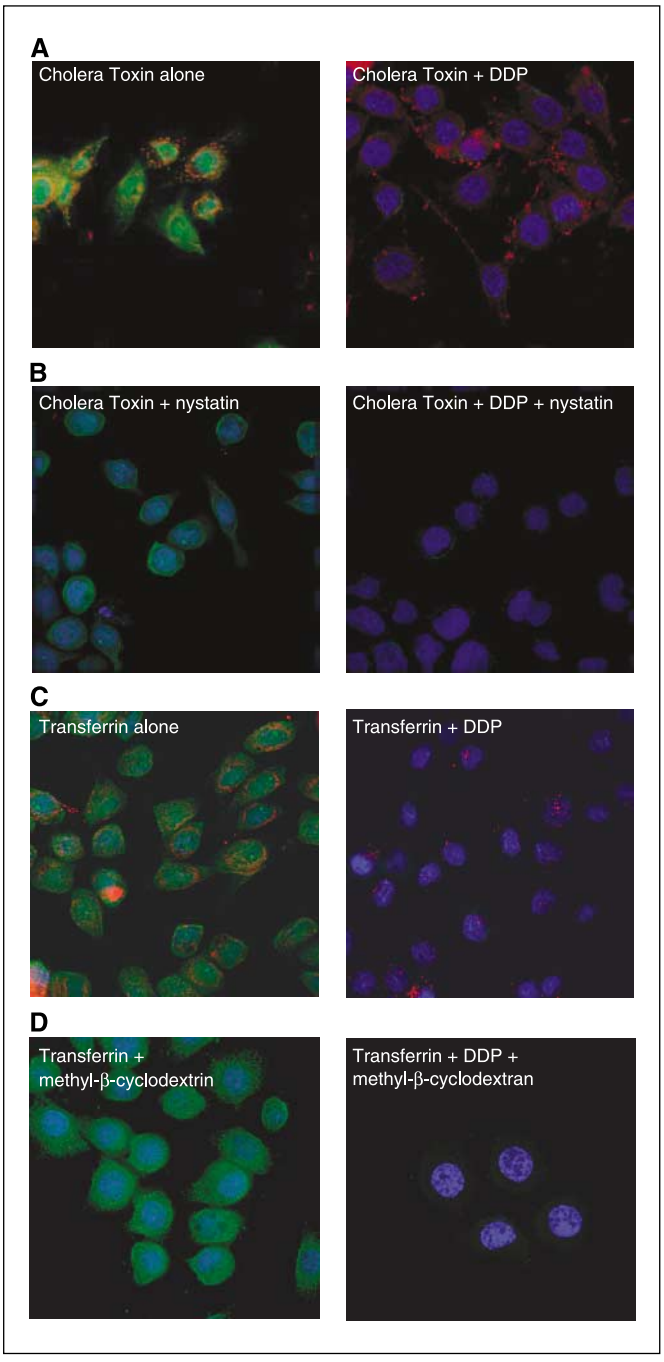

Figure 3. Confocal microscopic analysis of the effect of endocytotic pathway inhibitors nystatin and methyl-β-cyclodextrin on DDP-induced loss of hCTR1 from human ovarian carcinoma 2008 cells. In each case, following the indicated exposures, cells were stained for hCTR1 (*green*); Hoechst 33342 dye was used to label the nucleus (*blue*). *A,* untreated control cells incubated with Alexa Fluor 555–labeled cholera toxin B alone (*red; left*) and cells incubated with Alexa Fluor 555–labeled cholera toxin B and 2 μmol/L DDP for 15 minutes (*right*). *B,* cells incubated with Alexa Fluor 555–labeled cholera toxin B and exposed to 30 μg/mL nystatin for 30 minutes (*left*) and cells incubated with Alexa Fluor 555–labeled cholera toxin B and 30 μg/mL nystatin for 30 minutes and then 2 μmol/L DDP for 15 minutes (*right*). *C,* untreated control cells exposed to Alexa Fluor 546–labeled transferrin (*red; left*) and cells exposed to Alexa Fluor 546–labeled transferrin and 2 μmol/L DDP for 15 minutes (*right*). *D,* cells exposed to 3.5 mmol/L methyl-β-cyclodextrin for 30 minutes followed by Alexa Fluor 546–labeled transferrin (*left*) and cells exposed to 3.5 mmol/L methyl-β-cyclodextrin for 30 minutes followed by Alexa Fluor 546–labeled transferrin and then 2 μmol/L DDP for 15 minutes (*right*).

cells. However, as shown in Fig. 3*B* (compare *left* and *right*), blocking this pathway failed to prevent DDP-induced loss of hCTR1 from 2008 cells. The failure of nystatin to prevent down-regulation of hCTR1 expression was confirmed by Western blot analysis (Supplementary Fig. S3), and by staining with antibody to the COOH-terminal end of hCTR1 produced the same result (Supplementary Fig. S2).

Methyl-β-cyclodextrin is another compound that binds to cholesterol in membranes and blocks both caveolin- and clathrin-mediated endocytosis (25, 26). Transferrin is a well-recognized substrate for the clathrin-mediated pathway (24). As shown in Fig. 3 (compare *C* and *D*), a 30-minute exposure to 3.5 mmol/L methyl-β-cyclodextrin markedly reduced the accumulation of Alexa Fluor 546–labeled transferrin. However, as shown in Fig. 3*D*, it failed to block DDP-induced loss of hCTR1. This result was confirmed by Western blot analysis (Supplementary Fig. S3); it was further confirmed by showing that the same result was obtained with an antibody directed to a COOH-terminal hCTR1 epitope (Supplementary Fig. S2). Taken together, the results of the nystatin and methyl-β-cyclodextrin experiments indicate that clathrin- and caveolin-mediated endocytosis does not play a significant role in the DDP-induced disappearance of hCTR1.

Cells engineered to express dominant-negative forms of dynamin I or Rac1 were used to further test the dependence of DDP-induced loss of hCTR1 on the various endocytotic pathways. Dynamin I is essential for the pinching off of vesicles from the plasma membrane in many forms of endocytosis, including caveolin- and clathrin-mediated endocytosis as well as some clathrin- and caveolin-independent endocytotic processes and phagocytosis (23). The expression of a dominant-negative form of dynamin I, K44A, disables all forms of endocytosis, except for macropinocytosis. In this study, we used HeLa cells transfected with a tetracycline-repressible vector expressing the K44A variant of dynamin I bearing a hemagglutinin (HA) tag as previously reported (20). K44A dynamin I expression was induced by removing tetracycline for 48 hours, and then one aliquot of cells was exposed to 2 μmol/L DDP for 15 minutes, whereas the another was left untreated. To identify those cells in which the transdominant-negative dynamin I was successfully induced, both aliquots were exposed to Alexa Fluor 546–labeled transferrin before incubation with DDP; cells that express the K44A mutant do not accumulate transferrin. The cells were then fixed and stained for hCTR1. As shown in Fig. 4*A*, DDP induced the loss of hCTR1 in both cells that accumulated Alexa Fluor 546–labeled transferrin and those that did not, indicating that loss of hCTR1 was mediated by a dynamin I–independent process. To further show specificity, those cells in which the K44A dynamin I was expressed were directly identified by staining with an antibody for the HA tag appended to the mutant protein. Comparison of each image in Fig. 4*B* shows that DDP induced the loss of hCTR1 in both HA-positive and HA-negative cells. Similar results were obtained using an antibody to the COOH-terminal end of CTR1 (Supplementary Fig. S4). Both the loss of hCTR1 and the expression of the K44A mutant were verified by Western blot analysis (Supplementary Fig. S5). These results provide strong evidence that dynamin I–dependent mechanisms are not required for DDP-induced down-regulation of hCTR1.

Pinocytosis and other forms of endocytosis require the activity of the Rac GTPase, and these endocytotic pathways can be inhibited by expressing a dominant-negative form of Rac (27). The 2008 ovarian carcinoma cells were transiently transfected with a vector expressing the N17rac1 dominant-negative Rac bearing a myc tag

at the NH_2-terminal end (28). They were then exposed to Texas red–labeled 70-kDa dextran to permit identification of those cells in which pinocytosis and endocytosis had been successfully disabled by expression of the dominant-negative Rac1; one aliquot was also exposed to DDP, whereas a control aliquot was not. Both sets of cells were then stained for hCTR1. A comparison of the *left* and *right* of Fig. 4*C* indicates that, as it did in the nontransfected cells, DDP triggered loss of hCTR1 in cells expressing the Rac1 N17 dominant-negative vector and therefore not accumulating Texas red–labeled 70-kDa neutral dextran. Further evidence for specificity was provided by staining the DDP-treated and untreated cells for both hCTR1 and expression of the myc tag on the dominant-negative Rac. Figure 4*D* shows that DDP successfully down-regulated hCTR1 in both cells that expressed the mutant Rac and those that did not. These results support the conclusion that the loss of hCTR1 provoked by DDP is not dependent on a mechanism that requires Rac. These results were confirmed by showing that the same result was obtained with an antibody directed to a COOH-terminal hCTR1 epitope (Supplementary Fig. S4).

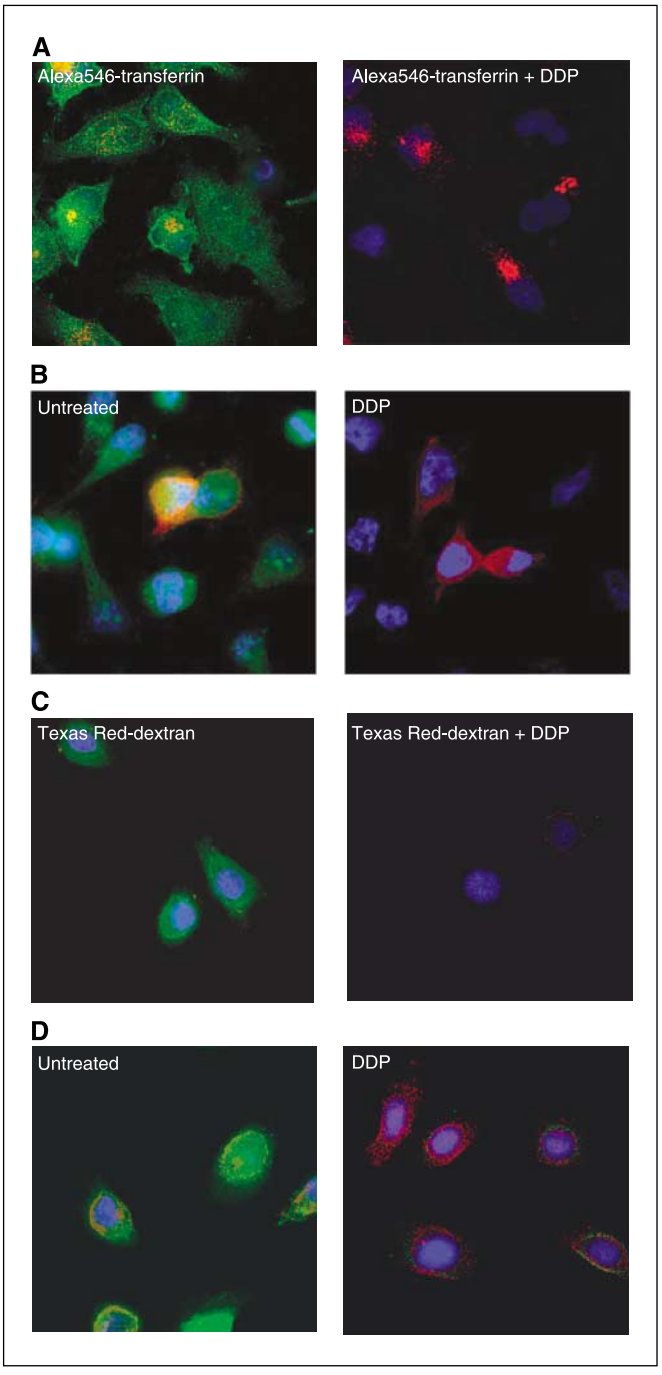

The results presented above identify macropinocytosis as the most important endocytotic pathway involved in the down-regulation of hCTR1 induced by clinically attainable concentrations of DDP. Plasma membrane proteins internalized by this route are frequently degraded in lysosomes (reviewed in ref. 29). However, some proteins internalized via macropinocytosis and phagocytosis undergo proteasomal degradation (30, 31). To determine the contribution of proteasomal degradation to the loss of hCTR1, 2008 cells were incubated with 2 μmol/L DDP in the presence or absence of several different proteasome inhibitors at concentrations shown not to produce significant cytotoxicity based on propidium iodide viability staining. The concentration of inhibitor selected was the lowest concentration that successfully blocked proteasomal degradation while maintaining cell viability.

As shown in Fig. 5*B* and *C*, inhibition of the trypsin- and chymotrypsin-like activities of the 20S proteasome with lactacystin prevented the loss of hCTR1 following DDP exposure. Likewise, inhibition of only the chymotrypsin-like portion of the 20S proteasome with proteasome inhibitor 1 also blocked the loss of hCTR1. Inhibition of the 26S portion of the proteasome responsible for degrading ubiquitin-conjugated proteins with MG132 also blocked the loss of hCTR1 on exposure to 2 μmol/L DDP. To verify these results and to ensure that the drugs were not just altering the epitope recognized by the NH_2-terminal antibody, all immunofluorescent results were verified using an antibody that recognized an epitope on the COOH-terminal end of hCTR1 (Supplementary Fig. S6). The results were also verified by Western blot analysis (Supplementary Fig. S7). Thus, although some component of hCTR1 degradation may occur in lysosomes, the majority of the rapid loss of hCTR1 from the cell seems to occur by proteasomal degradation.

To investigate the kinetics of the recovery of hCTR1 after DDP exposure, the time course of the reappearance of hCTR1 was

Figure 4. Confocal microscopic analysis of the effect of dominant-negative dynamin I and Rac on DDP-induced loss of hCTR1 loss. Anti-HA or anti-myc antibodies were used to identify the subset of cells in the population that expressed the K44A or Rac dominant-negative mutant. In each case, following the indicated exposures, cells were stained for hCTR1 (*green*); Hoechst 33342 dye was used to label the nucleus (*blue*). *A,* K44A-transfected control HeLa cells exposed to Alexa Fluor 546–labeled transferrin (*red*) to document inhibition of clathrin- and caveolin-mediated endocytosis (*left*) and K44A-transfected control HeLa cells exposed to Alexa Fluor 546–labeled transferrin for 30 minutes and then with 2 μmol/L DDP for 15 minutes (*right*). *B,* K44A-transfected control HeLa cells stained for the expression of the HA-tagged K44A dominant-negative mutant (*red; left*) and K44A-transfected control HeLa cells exposed to 2 μmol/L DDP for 15 minutes and stained for the expression of the HA-tagged K44A dominant-negative mutant (*right*). *C,* 2008 ovarian carcinoma cells transiently transfected with Rac1 N17 dominant-negative vector and incubated with Texas red–labeled 70-kDa neutral dextran to document inhibition of pinocytosis (*left*) and 2008 ovarian carcinoma cells exposed to 2 μmol/L DDP for 15 minutes following a transient transfection with Rac1 N17 dominant-negative vector and incubation with Texas red–labeled 70-kDa neutral dextran to document inhibition of pinocytosis (*right*). *D,* 2008 ovarian carcinoma cells transiently transfected with Rac1 N17 dominant-negative vector and stained for expression of the myc-tagged Rac1 N17 dominant-negative vector (*red; left*) and 2008 ovarian carcinoma cells exposed to 2 μmol/L DDP for 15 minutes following a transient transfection with Rac1 N17 dominant-negative vector and stained for expression of the myc-tagged Rac1 N17 dominant-negative vector (*red; right*).

monitored in 2008 cells following a 15-minute exposure to 2 μmol/L DDP. Both the absolute level and the subcellular localization were monitored by immunofluorescent microscopy (Fig. 6*A*) and Western blotting (Supplementary Fig. S8). hCTR1 protein levels returned to normal ~30 minutes after the removal of DDP, indicating that the synthesis of new hCTR1 protein is rapid. This conclusion was verified by blocking new hCTR1 synthesis with 100 μg/mL cyclohexamide. As shown in Fig. 6*B*, a 30-minute exposure to cyclohexamide reduced hCTR1 to undetectable levels, but normal levels were again achieved ~30 minutes after removal of the inhibitor. The findings were confirmed by Western blot analysis (Supplementary Fig. S9); it was further confirmed by showing that the same result was obtained with an antibody directed to a COOH-terminal hCTR1 epitope (Supplementary Fig. S10). These results indicate that hCTR1 is rapidly resynthesized, suggesting rapid turnover under steady-state conditions of synthesis and degradation.

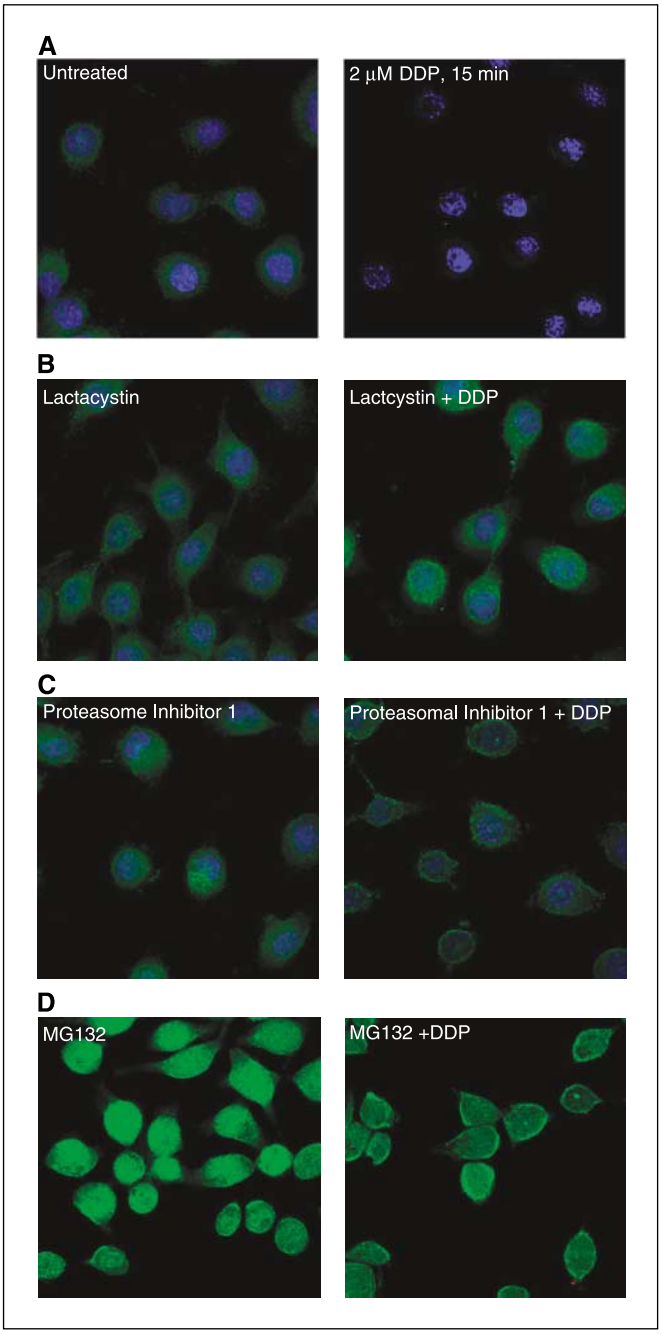

Figure 5. Confocal microscopic analysis of the effect of proteasomal inhibitors on DDP-induced down-regulation of hCTR1 in ovarian carcinoma 2008 cells. In each case, following the indicated exposures, cells were stained for hCTR1 (*green*); Hoechst 33342 dye was used to label the nucleus (*blue*). *A,* untreated control cells (*left*) and control cells exposed to 2 μmol/L DDP for 15 minutes (*right*). *B,* cells pretreated with 20 μmol/L lactacystin for 30 minutes (*left*) and cells pretreated with 20 μmol/L lactacystin for 30 minutes followed by exposure to 2 μmol/L DDP for 15 minutes (*right*). *C,* cells pretreated with 7 μmol/L proteasome inhibitor 1 for 30 minutes (*left*) and cells pretreated with 7 μmol/L proteasome inhibitor 1 for 30 minutes followed by exposure to 2 μmol/L DDP for 15 minutes (*right*). *D,* cells pretreated with 40 μmol/L MG132 for 30 minutes (*left*) and cells pretreated with 40 μmol/L MG132 for 30 minutes followed by exposure to 2 μmol/L DDP for 15 minutes (*right*).

Discussion

hCTR1 is important not only because it is the major copper influx transporter but also because it mediates a significant component of the cellular accumulation of DDP. As one step toward identifying how hCTR1 transports DDP, we sought to determine the mechanism by which endogenously expressed hCTR1 is degraded following brief exposure to DDP using several different strategies for inhibiting endocytotic pathways and proteasomal degradation. The results support the conclusion that the initial step of DDP-induced loss of hCTR1 from human ovarian carcinoma cells is mediated by a process that is inhibited by amiloride but not by nystatin or methyl-β-cyclodextrin and is not dependent on either dynamin I or the Rac1 GTPase. Among the various endocytotic pathways currently defined, this pattern of inhibition most closely matches the process of macropinocytosis.

As currently understood, macropinocytosis occurs through the formation of large primary endocytotic vesicles in regions of membrane ruffling. Although the specific mechanisms involved and controls on the process are not clearly defined, it is thought to be regulated by the small GTPase ARF6 and may be dependent on phospholipase Cγ activity. There is evidence that phosphatidylinositol (4, 5) bisphosphate is a regulator of the rate of macropinocytosis (32). However, whether macropinocytosis is triggered by interaction with molecules external to the cell or is a by-product of membrane turnover and cytoskeletal activity is currently a matter of debate (32). Unlike endosomes generated by clathrin- and caveolar-mediated endocytosis, macropinosomes do not fuse into lysosomes (33), suggesting that their cargo is not degraded by lysosomal enzymes (31). The observation that proteasome inhibitors blocked DDP-induced loss of hCTR1 is consistent with this concept. Several different proteasome inhibitors markedly reduced loss of hCTR1, indicating that proteasomal degradation accounts for the vast majority of hCTR1 breakdown and disappearance.

The specificity controls included in these studies provide strong evidence that the observed disappearance of hCTR1 from the cell following DDP and copper exposure was not an artifact. Two separate antibodies directed at opposite ends of the protein detected the same time course of the loss and recovery of hCTR1 in immunofluorescent studies. Yet, another antibody, capable of detecting hCTR1 on Western blots, also showed a similar temporal pattern. Thus, it is unlikely that loss of hCTR1 was due to epitope masking. In addition, DDP did not seem to cause a general disturbance in the function of endocytotic pathways, as there was no disturbance of the cellular accumulation of transferrin, cholera toxin B, or dextran in the DDP-treated cells. Whereas treatment

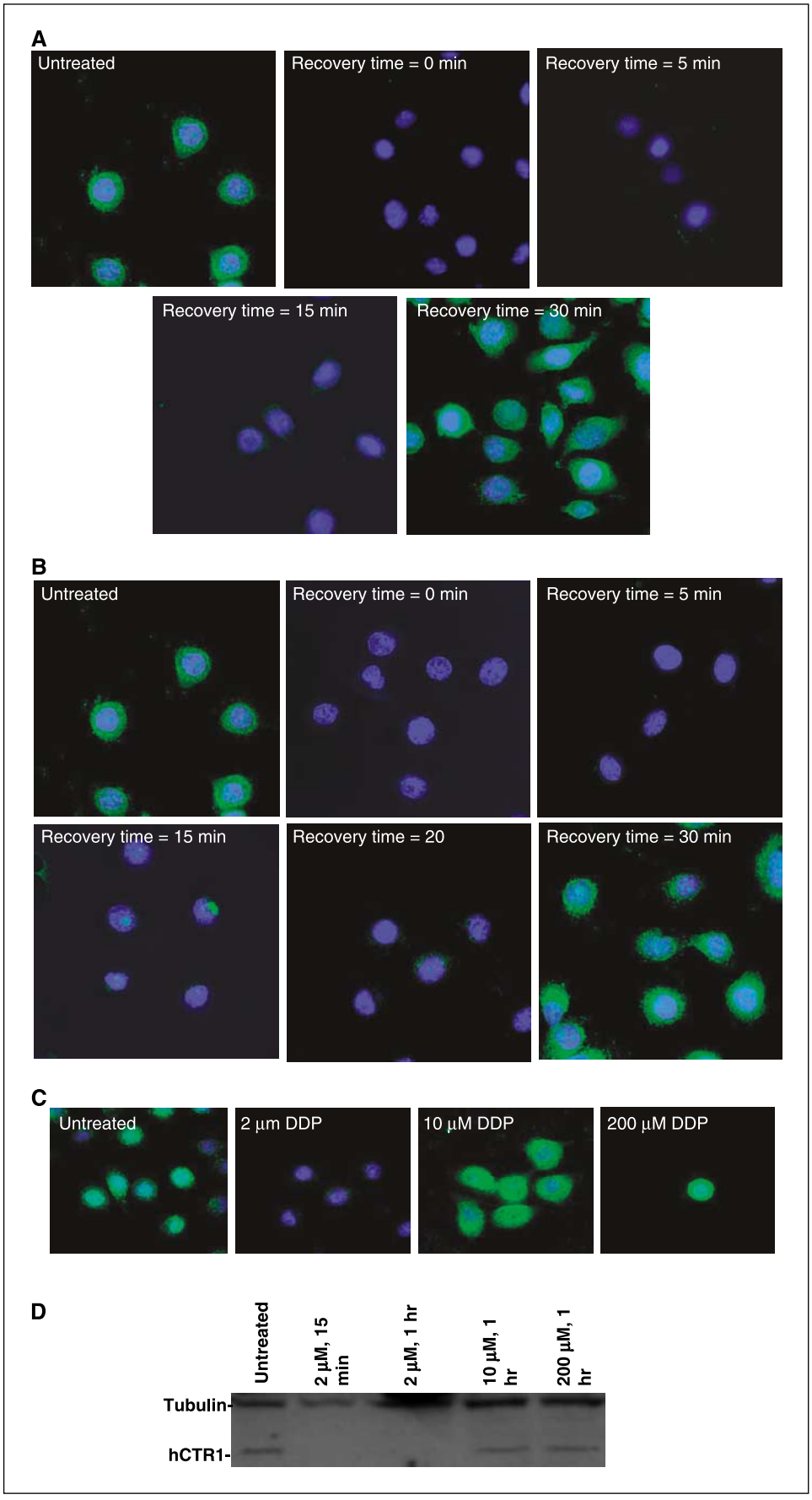

Figure 6. Confocal microscopic analysis of the recovery of hCTR1 following DDP exposure in 2008 ovarian carcinoma cells and hCTR1 levels following exposure to high DDP concentrations. *A,* 2008 ovarian carcinoma cells were exposed to 2 μmol/L DDP for 15 minutes. Following removal of the DDP, cells were allowed to recover for 0, 5, 15, or 30 minutes before fixation. Cells were then stained for hCTR1 (*green*) and with Hoechst 33342 to label the nucleus (*blue*). *B,* 2008 ovarian carcinoma cells were exposed to 100 μg/mL cyclohexamide for 30 minutes and then allowed to recover for 0, 5, 15, 20, or 30 minutes before fixation. Cells were then stained for hCTR1 (*green*) and with Hoechst 33342 to label the nucleus (*blue*). *C,* 2008 ovarian carcinoma cells exposed to 0, 2, 10, and 200 μmol/L DDP for 1 hour. Cells were then stained for hCTR1 (*green*) and with Hoechst 33342 to label the nucleus (*blue*). *D,* Western blot showing the expression of tubulin and hCTR1 in 2008 ovarian carcinoma cells exposed to 0, 2, 10, and 200 μmol/L DDP for 1 hour, except where listed. Blot is representative of three independent analyses done with lysates from three independent experiments.

with DDP did not significantly alter endocytosis, treatment with the various endocytotic inhibitors did alter the overall expression levels of hCTR1 in treated cells. This is most likely due to disruption of the normal cycling pattern of hCTR1. Chemical endocytotic inhibitors are not specific and can result in the alteration of numerous cellular functions, which could affect the overall level of hCTR1. hCTR1 seems to be a tightly regulated protein, so one would expect several different cellular processes to play a role in its localization and expression levels in the cell.

The studies reported here are consistent with the concept that, in the absence of excessively high copper levels or DDP exposure, hCTR1 resides largely in membranes where it is protected from proteasomal degradation. Inhibition of the entire proteasome resulted in an increase of overall hCTR1 levels, indicating that hCTR1 is regulated in part by proteasomal degradation. The rapid loss of hCTR1 when new protein synthesis was inhibited suggests that basal rates of macropinocytosis internalize hCTR1 at a relatively high rate and make it accessible to degradation by the proteasome. Both brief exposure to DDP and inhibition of new protein synthesis with cyclohexamide rapidly reduced the level of hCTR1 to below the limit of detection. The recovery of hCTR1 levels over the ensuing ~30 minutes following either exposure to DDP or cyclohexamide indicates that hCTR1 is rapidly resynthesized and trafficked to its normal cellular membrane locations. The available data support the idea that, in ovarian cancer cells, both copper and DDP markedly increase the rate of hCTR1 internalization by macropinocytosis, thus enhancing proteasomal degradation, although on a molar basis DDP is far more effective than copper at triggering this effect. How either metalloid actually accomplishes this remains unknown. It seems likely that binding to the metal-binding motifs located in the NH_2-terminal extracellular portion of hCTR1 causes a conformational change that marks the protein for loading into macropinosomes, but this has yet to be established.

The results reported here, and in a previous article (16), using ovarian carcinoma cells differ importantly from a previous report of the effect of DDP on hCTR1 overexpressed in transfected kidney HEK293 cells. Guo et al. (34) reported that, when examined at the end of a 1- to 6-hour exposure to an extremely high concentration of DDP (50-1,000 μmol/L), rather than undergoing degradation hCTR1 rapidly formed a high molecular weight complex via interactions between the DDP and the methionine-containing motifs in the NH_2-terminal region of the protein and that this complex remained associated with cellular membranes. Why hCTR1 behaves differently in kidney and ovarian carcinoma cells is not yet clear. However, it is important to note that the concentrations of DDP used by Guo et al. were way above those attainable in the plasma of patients receiving DDP therapy (35) and that at these concentrations DDP is known to produce extensive cross-linking of intracellular proteins (36). As shown in Fig. 6*C* and *D*, we have confirmed that a 1-hour exposure to such high concentrations of DDP also blocks the disappearance of hCTR1 from ovarian carcinoma 2008 cells; however, there is concern that this is an artifact unrelated to the response of hCTR1 to DDP concentrations actually attained in tumors during therapy.

Although the effect of DDP on hCTR1 has now been examined in several systems, the fate of the DDP that is presumably bound to it, or transported by it, has yet to be determined. Previous reports illustrate that hCTR1 does in fact deliver DDP into the cell (10–12), but where it traffics in the cell and how it reaches the DNA is unknown. Studies done in CTR1-null cells suggest that 65% of the platinum accumulation that occurs when cells are exposed to 2 μmol/L DDP enters the cell via CTR1 (37). The results presented here suggest that hCTR1 can contribute to the influx of DDP over the first few minutes; however, because it rapidly disappears from the cell, some other hCTR1-independent uptake process must be responsible for the subsequent cellular accumulation of DDP, which continues for several hours until steady-state levels are attained (10). In future studies, it will be of substantial interest to determine whether amiloride or proteasomal inhibitors can be used to pharmacologically enhance DDP uptake selectively into those tumors that express large amounts of hCTR1.

Acknowledgments

Received 5/11/2006; revised 7/22/2006; accepted 8/28/2006.

Grant support: NIH grant CA95298, Department of Defense grant DAMD17-03-1-0158, and Clayton Foundation for Medical Research.

The costs of publication of this article were defrayed in part by the payment of page charges. This article must therefore be hereby marked *advertisement* in accordance with 18 U.S.C. Section 1734 solely to indicate this fact.

We thank J. Wadia and S.F. Dowdy for their assistance in experimental design and for providing the dominant-negative mutant vectors, Dr. Leo Klomp for providing the NH_2-terminal hCTR1 antibody used in some of the immunofluorescent studies, S. Schmid for providing K44A-transfected HeLa cell line, and Michael Petris for helpful discussions.

References

1. Gonzalez VM, Fuertes MA, Alonso C, Perez JM. Is cisplatin-induced cell death always produced by apoptosis? Mol Pharmacol 2001;59:657–63.
2. Andrews PA, Howell SB. Cellular pharmacology of cisplatin: perspectives on mechanisms of acquired resistance. Cancer Cell 1990;2:35–43.
3. Andrews PA, Jones JA, Varki NM, Howell SB. Rapid emergence of acquired *cis*-diamminedichloroplatinum(ii) resistance in an *in vivo* model of human ovarian carcinoma. Cancer Commun 1990;2:93–100.
4. Gately DP, Howell SB. Cellular accumulation of the anticancer agent cisplatin: a review. Br J Cancer 1993;67:1171–6.
5. Safaei R, Howell SB. Copper transporters regulate the cellular pharmacology and sensitivity to Pt drugs. Crit Rev Oncol Hematol 2005;53:13–23.
6. Pena MM, Lee J, Thiele DJ. A delicate balance: homeostatic control of copper uptake and distribution. J Nutr 1999;129:1251–60.
7. Katano K, Kondo A, Safaei R, et al. Acquisition of resistance to cisplatin is accompanied by changes in the cellular pharmacology of copper. Cancer Res 2002;62:6559–65.
8. Safaei R, Katano K, Samimi G, et al. Cross-resistance to cisplatin in cells with acquired resistance to copper. Cancer Chemother Pharmacol 2004;53:239–46.
9. Lin X, Okuda T, Holzer A, Howell SB. The copper transporter CTR1 regulates cisplatin uptake in *Saccharomyces cerevisiae*. Mol Pharmacol 2002;62:1154–9.
10. Holzer AK, Samimi G, Katano K, et al. The copper influx transporter human copper transport protein 1 regulates the uptake of cisplatin in human ovarian carcinoma cells. Mol Pharmacol 2004;66:817–23.
11. Ishida S, Lee J, Thiele DJ, Herskowitz I. Uptake of the anticancer drug cisplatin mediated by the copper transporter Ctr1 in yeast and mammals. Proc Natl Acad Sci U S A 2002;99:14298–302.
12. Song IS, Savaraj N, Siddik ZH, et al. Roles of copper transporter Ctr1 in the transport of platinum-based antitumor agents in cisplatin-sensitive and resistant cells. Mol Cancer Ther 2004;3:1543–9.
13. Petris MJ. The SLC31 (Ctr) copper transporter family. Pflugers Arch 2004;447:752–5.
14. Petris MJ, Smith K, Lee J, Thiele DJ. Copper-stimulated endocytosis and degradation of the human copper transporter, hCtr1. J Biol Chem 2003;278:9639–46.
15. Ooi CE, Rabinovich E, Dancis A, Bonifacino JS, Klausner RD. Copper-dependent degradation of the *Saccharomyces cerevisiae* plasma membrane copper transporter Ctr1p in the apparent absence of endocytosis. EMBO J 1996;15:3515–23.
16. Holzer AK, Katano K, Klomp LW, Howell SB. Cisplatin rapidly down-regulates its own influx transporter hCTR1 in cultured human ovarian carcinoma cells. Clin Cancer Res 2004;10:6744–9.
17. Klomp AE, Tops BB, Van Denberg IE, Berger R, Klomp LW. Biochemical characterization and subcellular localization of human copper transporter 1 (hCTR1). Biochem J 2002;364:497–505.
18. Hamilton TC, Winker MA, Louie KG, et al. Augmentation of adriamycin, melphalan, and cisplatin cytotoxicity by buthionine sulfoximine depletion of glutathione in drug resistant human ovarian cancer. Proc Am Assoc Cancer Res 1985;26:345–7.
19. Disaia PJ, Sinkovics JG, Rutledge FN, Smith JP. Cell-mediated immunity to human malignant cells. Am J Obstet Gynecol 1972;114:979–89.

20. Damke H, Baba T, Warnock DE, Schmid SL. Induction of mutant dynamin specifically blocks endocytic coated vesicle formation. J Cell Biol 1994;127:915–34.

21. Araki N, Johnson MT, Swanson JA. A role for phosphoinositide 3-kinase in the completion of macropinocytosis and phagocytosis by macrophages. J Cell Biol 1996;135:1249–60.

22. Oliver JM, Berlin RD, Davis BH. Use of horseradish peroxidase and fluorescent dextrans to study fluid pinocytosis in leukocytes. Methods Enzymol 1984;108: 336–47.

23. Conner SD, Schmid SL. Regulated portals of entry into the cell. Nature 2003;422:37–44.

24. Riezman H, Woodman PG, van Meer G, Marsh M. Molecular mechanisms of endocytosis. Cell 1997;91:731–8.

25. Rodal SK, Skretting G, Garred O, Vilhardt F, van Deurs B, Sandvig K. Extraction of cholesterol with methyl-β-cyclodextrin perturbs formation of clathrin-coated endocytic vesicles. Mol Biol Cell 1999;10:961–74.

26. Subtil A, Gaidarov I, Kobylarz K, Lampson MA, Keen JH, McGraw TE. Acute cholesterol depletion inhibits clathrin-coated pit budding. Proc Natl Acad Sci U S A 1999;96:6775–80.

27. Burridge K, Wennerberg K. Rho and Rac take center stage. Cell 2004;116:167–79.

28. Ridley AJ, Paterson HF, Johnston CL, Diekmann D, Hall A. The small GTP-binding protein rac regulates growth factor-induced membrane ruffling. Cell 1992;70:401–10.

29. Peters C, von Figura K. Biogenesis of lysosomal membranes. FEBS Lett 1994;346:108–14.

30. Zhou Y, Bosch ML, Salgaller ML. Current methods for loading dendritic cells with tumor antigen for the induction of antitumor immunity. J Immunother 2002; 25:289–303.

31. Johannes L, Lamaze C. Clathrin-dependent or not: is it still the question? Traffic 2002;3:443–51.

32. Nichols BJ, Lippincott-Schwartz J. Endocytosis without clathrin coats. Trends Cell Biol 2001;11:406–12.

33. Wadia JS, Stan RV, Dowdy SF. Transducible TAT-HA fusogenic peptide enhances escape of TAT-fusion proteins after lipid raft macropinocytosis. Nat Med 2004;10:310–5.

34. Guo Y, Smith K, Petris MJ. Cisplatin stabilizes a multimeric complex of the human Ctr1 copper transporter: requirement for the extracellular methionine-rich clusters. J Biol Chem 2004;279:46393–9.

35. Urien S, Brain E, Bugat R, et al. Pharmacokinetics of platinum after oral or intravenous cisplatin: a phase 1 study in 32 adult patients. Cancer Chemother Pharmacol 2005;55:55–60.

36. Filipski J, Kohn KW, Bonner WM. Differential cross-linking of histones and non-histones in nuclei by cis-Pt(ii). FEBS Lett 1983;152:105–8.

37. Holzer AK, Manorek GH, Howell SB. The role of the copper transport protein 1 in the cellular accumulation of cisplatin, oxaliplatin, and carboplatin. Proc Am Assoc Cancer Res 2006;47:311.